

Collisional radiative model for M1 transition spectrum of the highly-charged W^{54+} ions

Xiaobin Ding^{a,b,*}, Jiaoxia Yang^a, Linfan Zhu^b, Fumihiro Koike^c, Izumi Murakami^{d,e}, Daiji Kato^{d,e,f}, Hiroyuki A Sakaue^d, Nobuyuki Nakamura^g, Chenzhong Dong^{a,*}

^a*Key Laboratory of Atomic and Molecular Physics and Functional Materials of Gansu Province, College of Physics and Electronic Engineering, Northwest Normal University, Lanzhou 730070, China*

^b*Hefei National Laboratory for Physical Sciences at Microscale and Department of Modern Physics, University of Science and Technology of China, Hefei, Anhui 230026, China*

^c*Department of physics, Sophia University, Tokyo 102-8554, Japan*

^d*National Institute for Fusion Science, National Institutes of Natural Sciences, Toki, Gifu 509-5292, Japan*

^e*Department of Fusion Science, SOKENDAI, Toki, Gifu, 509-5292, Japan*

^f*Department of Advanced Energy Engineering Science, Kyushu University, Kasuga, Fukuoka, 816-8580, Japan*

^g*Institute for Laser Science, The University of Electro-Communications, Chofu, Tokyo 182-8585, Japan*

Abstract

A detailed-level collisional-radiative model for the M1 transition spectrum from the electron beam ion trap (EBIT) experiment of the Ca-like W^{54+} ion was constructed based on the atomic data obtained by the relativistic configuration interaction (RCI) method and distorted wave theory. The present calculated transition energy, rate and intensity of the M1 transitions of W^{54+} ions are compared with the previous theoretical values. The results are in reasonable agreement with the available experimental and theoretical data. The synthetic spectrum successfully explained the EBIT spectrum in 12-20 nm region, while a new possible strong transition has been predicted to be observable in an appropriate electron beam energy. The present work provided accurate atomic data and might be used for further plasma diagnostics application.

Keywords: Collisional-radiative model, Ca-like Tungsten, Relativistic

*Corresponding author.

Email addresses: dingxb@nwnu.edu.cn (Xiaobin Ding), dongcz@nwnu.edu.cn (Chenzhong Dong)

1. Introduction

The structures and properties of tungsten ions draw more and more attention in recent research due to its close relation to the magnetic confined fusion. Tungsten has been chosen to be the armour material of the plasma-facing component or the divertor in various fusion reactor, such as ITER, EAST, JET, ASDEX-Upgrade etc., because of its favourable physical, chemical and engineering-thermal physics properties such as the ability to withstand high heat loads, lower sputtering yield and tritium retention[1, 2]. Therefore, the tungsten ions as an intrinsic impurity ions will be inevitably produced due to the interaction between the edge plasma and the plasma facing-component and possibly be transported into the hot core plasma region. However, as a heavy element with many electrons, the tungsten ions could not be fully ionized even in the core plasma with high temperature ($T_e \sim 25$ keV) of ITER. These highly charged ions will emit high energy photon. Thus, large radiation loss from these ions could be expected, which will lead to the disruption of the plasma if the relative concentration of W ion impurities in the core plasma is higher than about 10^{-5} [3]. Monitoring and controlling the flux of the highly charged W impurity ions will be crucial to the success of the fusion[4]. Furthermore, the spectra of W impurity ions observed from the fusion plasma can be used as one of the most important diagnostic tools to measure the electron density and temperature of the plasma.

There are many research works on the radiative properties of tungsten ions related to fusion in various ionization stage in the past several decades[5–13]. Among these works special attention had paid to the magnetic dipole (M1) transition of W^{54+} ion [14–21]. Y. Ralchenko *et al* observed two transition peaks at 14.986 nm and 17.144 nm in the wavelength range 10-20 nm of the M1 transition among the ground configuration $[Ne]3s^23p^63d^2$ multiplets for W^{54+} ion from the EBIT (electron beam ion trap) experiment[15]. They also observed another

weaker transition peak of the same ion in the later work, and a non-Maxwellian collisional-radiative model was employed to analyse the observed spectrum[14]. U. I. Safronova *et al*[19] calculated the M1 transitions between the multiplets of the ground state configuration ($[\text{Ne}]3s^23p^63d^2$) of W^{54+} by using the relativistic many-body perturbation theory (RMBPT). P. Quinet[20] calculated the wavelengths and transition rates of the forbidden transition of the $3d^n$ ($n=1-9$) and $3d^k$ ($k=1,5$) ground configuration of tungsten ions (W^{47+} - W^{61+}) by full relativistic Dirac-Fock method. Guo *et al*[21] calculated the energy, transition wavelengths and rates for M1 forbidden transition of W^{54+} ion by the RMBPT and relativistic configuration interaction method. Ding *et al*[16-18] calculated the E1, E2, M1, M2 transitions data (the wavelengths, energy levels, radiative transition rates) of W^{54+} ion by using the Multi-Configuration Dirac Fock (MCDF) method with restricted active space method. The results were in comprehensive and reasonable agreement with available experimental and theoretical values. They also constructed a detailed-level collisional-radiative model to simulate the visible spectrum of the M1 transition of W^{26+} [22] and the soft X-ray spectrum of the E1 transition of W^{54+} [23] ions which had been observed in various EBIT experiment. The present work is devoted to explain the observation of M1 spectrum from the previous EBIT experiment[14, 15].

2. Theoretical method

Collisional-Radiative modeling has been successfully used to analyze the plasma spectrum. In the observed plasma spectrum, the intensity $I_{i,j}(\lambda)$ of an individual transition, which due to a radiative transitions with wavelength λ from the upper level i to the lower level j of the ion in an optically thin plasma, is proportional to the transition energy $h\nu$, transition rate $A(i,j)$, the population of the ions in the upper excited level i $n(i)$ and the normalized line profile $\phi(\lambda)$, which can be wrote as:

$$I_{i,j}(\lambda) \propto n(i)h\nu A(i,j)\phi(\lambda) \quad (1)$$

where the normalized line profile $\phi(\lambda)$ was taken as a Gaussian profile, which may include the effect of Doppler, natural, collisional and instrumental broadening in the observation. The population of upper excited level $n(i)$ is determined by various atomic physics processes in the plasma such as spontaneous radiative transition, electron collisional (de)excitation, radiative recombination, electron collisional ionization, dielectronic recombination, three-body recombination and some other interaction processes between atom and ion, ion and ion etc.. The free electron energy distribution in the electron beam of an EBIT facility is mostly mono-energy under typical operation conditions. And the excited state population was mostly determined by the collisional (de)excitation process. Thus, in the present calculation only the spontaneous radiative transition and collisional (de)excitation processes are taken into account. The effects of the radiative recombination, dielectronic recombination, three body recombination, electron collisional ionization and other processes are expected to be negligible in the cases of current interest because they only slightly affect the population of the low-lying levels.

The temporal development of the population $n(i)$ in a specific excited level i can be obtained by solving the collisional-radiative rate equation:

$$\begin{aligned} \frac{d}{dt}n(i) = & \sum_{j < i} C(i, j)n_e n(i) \\ & - [\sum_{j < i} F(i, j)n_e + A(i, j) + \sum_{j > i} C(i, j)n_e]n(i) \\ & + \sum_{j > i} [F(j, i)n_e + A(j, i)]n(j) \end{aligned} \quad (2)$$

where n_e is the electron density of the plasma, $C(i, j)$ and $F(j, i)$ are collisional excitation and deexcitation rate coefficients from the level j to i , respectively. The collisional excitation rate coefficient can be calculated by convoluting the cross section of the collisional excitation process with the free electron energy distribution function. For the plasma with the electron temperature T_e , the free electron energy distribution function was assumed as Maxwellian distribution. For the EBIT facility, the free electron energy distribution is more like mono-energy distribution function that can be taking as the δ function. The collisional

dexcitation rate coefficients can be obtained by the detailed balance principle. These rate equations are solved under the Quasi-Steady-State (QSS) approximation, i.e., $dn(i)/dt = 0$. Under this approximation, the intensity $I_{i,j}(\lambda)$ of the spectrum of transition lines can be calculated when the population $n(i)$ of the transition is obtained.

W^{54+} ion is a highly charged ion and the ground state is $[Ne]3s^23p^63d^2$ which have two electrons in the outmost 3d subshells. In order to construct the appropriate CR model for the M1 spectrum of W^{54+} ion, all the levels of the configuration by single and double electron substitution from $n=3$ to $n=4$ subshells were included. There are 2,078 levels in the present CRM. The configuration interaction effects were taken into account by the same scheme in our previous work[23] which was valid to describe the most important electron correlation effects in W^{54+} ion. All the necessary fundamental atomic data such as the energy levels, radiative transition rates (E1, M1, E2, M2), and cross sections of collision (de)excitation were calculated by the full relativistic configuration interaction method and distorted wave method with the implementation of Flexible Atomic Code (FAC) packages[24].

3. Result and discussion

The transition wavelength λ (in nm), transition rate A (in s^{-1}), population of the upper excited level $n(i)$ and the intensity (emission power density of the plasma) Int. of the M1 transition among the ground state $3s^23p^63d^2$ multiplets of W^{54+} ion are presented in Table 1. " λ_{Exp} " and " λ_{Theo} " represents the results from the EBIT experiment and other theory, such as MCDF, RMBPT and RCI methods, respectively. It can be found from the table that the calculated wavelengths and transition rates are all in reasonable agreement with available experimental and others theoretical results. The discrepancy of the transition wavelength between present calculation and the EBIT experimental observation is within 0.34%. In the previous MCDF calculation, P. Quinet *et al*[20] took the electron correlation among the $n = 3$ complex and some $n = 3$ to $n = 4$

single excitation configuration into account. The discrepancies of the transition wavelengths and rates with the present calculation are about 0.07% and 0.01%, respectively. Ding *et al*[18] have included electron correlation a little more by extend the correlation configuration to the $n = 3$ complex and the single and double excitation to $n = 6$ subshells, and the discrepancies of the transition wavelengths and rates with the present calculation are about 0.02% and 0.03%, respectively. U. I. Safranova and A. S. Safranova[19] started their calculation from the Dirac-Fock potential of $1s^2 2s^2 2p^6 3s^2 3p^6$ for Ca-like tungsten ion by RMBPT. The discrepancies of the transition wavelengths and rates with the present calculation are about 0.24% and 0.58%, respectively. This large discrepancies are mainly due to the correlation effects of the 3s and 3p orbitals which were omitted in the RMBPT calculation. Y. Ralchenko *et al.* calculated the energy levels and the M1 transition rates of the ground state of W^{54+} ion by FAC. The configuration interaction among $n = 3$ complex and the single excitation up to $n = 5$ were taken into account in their calculation[14]. Both the transition wavelength and rate agree very well with the present work by about 0.02% and 0.01%, respectively. In order to ensure the completeness, the configuration interaction between $n = 3$ complex and the single and double excitation to $n = 4$ have been included more extensively in the present calculation. From the data of the intensity $I_{i,j}$ in Table 1, only these transitions with large intensity could be observed in the experiment. Some of the transitions which have large transition rates but small population will lead to small intensity which can not be observed in the present electron beam energy and density of electrons.

The synthetic spectrum for the M1 transitions of the ground configuration of W^{54+} ion in the wavelength range 12-20 nm is shown in Fig. 1. The upper panel(Fig. 1(a)) is the spectrum obtained by convoluting the transition rates directly with the Gaussian profile which shows the relative magnitude of the transition rates. The middle panel (Fig. 1(b)) is the spectrum for the EBIT case with the electron density $n_e = 10^{10} \text{ cm}^{-3}$ and the electron beam energy $E_e = 6000 \text{ eV}$. In the present calculation, all the observed transition lines in the EBIT experiment[14] were reproduced, such as the transition with key 4,

8 and 10. In addition to these three strong transitions, the peak 3 is observable in the future EBIT experiment with the same operation condition. This transition (key 3) was assigned to the M1 transition $(3/2, 3/2)_2 \rightarrow (3/2, 5/2)_1$ of the ground configuration of the W^{54+} ion with wavelength 14.154 nm. The bottom panel (Fig. 1(c)) is the spectrum by considering in the plasma with the electron density $n_e = 10^{16} \text{ cm}^{-3}$ and the electron temperature $T_e = 6000 \text{ eV}$, and the free electron energy distribution is Maxwellian. The results indicates that all transitions with large transition probabilities would be observed in this condition.

The intensity for a specific transition is proportion to the population of the excited upper level i and transition rates. In general, the transition with larger transition rates will be possibly observed in the experiment. However, in the present case, the transition with key 1 which has larger transition rates but wasn't observed in the previous experiment, while another transition with key 4 was observed in the experiment which has slightly smaller transition rate as shown in Fig 1 (a) and (b). It is clear in the calculation, for the transition with key 4, the ratio of the population flux and depopulation flux is 11.69, while for the weak one with the key 1 the ratio of the population flux and depopulation flux is only 0.107. This lead to a significant decrease of the population of the upper excited level of the transition with the key 1.

4. Conclusion

A collisional-radiative model (CRM) for M1 spectrum of W^{54+} ion which observed in the EBIT experiment was constructed by considering the spontaneous radiative transition, electron collisional (de)excitation processes in the plasma. The transition wavelength and transition rates of the ground configuration $3s^23p^63d^2$ of W^{54+} ion were calculated using relativistic configuration interaction method. All the necessary atomic data for constructing the CRM was calculated by FAC packages. The calculated energy levels and transition rates made a reasonable agreement with the previous theoretical and exper-

Table 1. The calculated transition wavelength λ (nm), transition rate A (s^{-1}), population $n(i)$, intensity $\text{Int.}(\text{eV cm}^{-3} \text{ s}^{-1})$ and available experimental and other theoretical values for the strong M1 transition of W^{54+} ion. The column 'Key' correspond to the label in Fig 1. Notion $a(b)$ for transition rates A means $a \times 10^b$.

Lower	Upper	$\lambda(nm)$	$\lambda_{Exp}(\text{nm})$	$\lambda_{Theo.}(\text{nm})$	$A(\text{s}^{-1})$	$A_{othe.}(\text{s}^{-1})$	$n(i)$	$\text{Int.}(\text{eV cm}^{-3} \text{ s}^{-1})$	Key
$(3/2, 3/2)_2$	$(5/2, 5/2)_2$	7.703		$7.712^b 7.694^c$	1.18(4)	$1.28(4)^b 1.15(4)^c$	1.96E-23	5.83E-11	
$(3/2, 5/2)_1$	$(5/2, 5/2)_0$	12.720		$12.721^b 12.723^c$	7.85(6)	$7.32(6)^b 7.88(6)^c$	8.32E-10	9.91E+05	1
				12.757 ^d		7.83(6) ^d			
$(3/2, 5/2)_3$	$(5/2, 5/2)_2$	13.987		$14.008^b 13.981^c$	7.57(5)	$7.52(5)^b 7.59(5)^c$	1.96E-23	2.06E-09	2
$(3/2, 3/2)_2$	$(3/2, 5/2)_1$	14.154		$14.176^b 14.150^c$	2.62(5)	$2.58(5)^b 2.63(5)^c$	2.73E-06	9.82E+07	3
$(3/2, 3/2)_2$	$(3/2, 5/2)_2$	14.986	14.959 ^a	14.984 ^a	1.81(6)	$1.80(6)^a 1.80(6)^b$	2.27E-06	5.30E+08	4
				15.010 ^b 14.974 ^c		1.82(6) ^c 1.81(6) ^d			
				14.980 ^d		1.77(6) ^e			
				(14.970, 14.924) ^e					
$(3/2, 5/2)_3$	$(5/2, 5/2)_4$	15.380		$15.413^b 15.369^c$	3.82(6)	$3.76(6)^b 3.84(6)^c$	2.35E-08	1.13E+07	5
				15.369 ^d		3.82(6) ^d			
$(3/2, 5/2)_2$	$(5/2, 5/2)_2$	15.849		$15.860^b 15.827^c$	3.11(6)	$3.10(6)^b 3.13(6)^c$	1.96E-23	7.44E-09	6
				15.848 ^d		3.11(6) ^d			
$(3/2, 5/2)_1$	$(5/2, 5/2)_2$	16.899		$16.911^b 16.865^c$	1.30(6)	$1.29(6)^b 1.31(6)^c$	1.96E-23	2.93E-09	7
				16.907 ^d		1.30(6) ^d			
$(3/2, 3/2)_2$	$(3/2, 5/2)_3$	17.144	17.080 ^a	17.147 ^a	3.68(6)	$3.68(6)^a 3.68(6)^b$	2.27E-06	9.43E+08	8
				17.157 ^b 17.110 ^c		3.70(6) ^c 3.68(6) ^d			
				17.138 ^d		3.64(6) ^e			
				(17.071, 17.218) ^e					
$(3/2, 5/2)_4$	$(5/2, 5/2)_4$	18.607		$18.593^b 18.553^c$	1.10(6)	$1.11(6)^b 1.10(6)^c$	2.35E-08	2.68E+06	9
				18.621 ^d		1.09(6) ^d			
$(3/2, 3/2)_0$	$(3/2, 5/2)_1$	19.268	19.177 ^a	19.281 ^a	1.72(6)	$1.72(6)^a 1.77(6)^b$	2.73E-06	4.74E+08	10
				19.294 ^b 19.218 ^c		1.74(6) ^c 1.74(6) ^d			
				19.222 ^d		1.71(6) ^e			
				(19.160, 19.422) ^e					
$(3/2, 5/2)_3$	$(3/2, 5/2)_4$	88.692		$90.123^b 89.579^c$	8.78(3)	$8.56(3)^b 8.49(3)^c$	4.34E-04	5.31E-01	
$(3/2, 5/2)_3$	$(3/2, 5/2)_2$	119.045		119.974 ^b	4.52(3)	$4.35(3)^b 4.43(3)^c$	2.27E-06	1.65E+05	
				119.920 ^c					
$(3/2, 5/2)_2$	$(3/2, 5/2)_1$	255.047		255.066 ^b	6.71(2)	$6.79(2)^b 6.57(2)^c$	2.35E-06	1.19E+04	
				255.047 ^c					

^a From Y. Ralchenko et al by an electron-beam ion trap (EBIT) and an non-Maxwellian collisional-radiative model[14].

^b From U. I. Safronova and A. S. Safronova by RMBPT method[19].

^c From Ding et al by MCDF method[18].

^d From P. Quinet by MCDF method[20].

^e From Guo et al by RMBPT and RCI method[21].

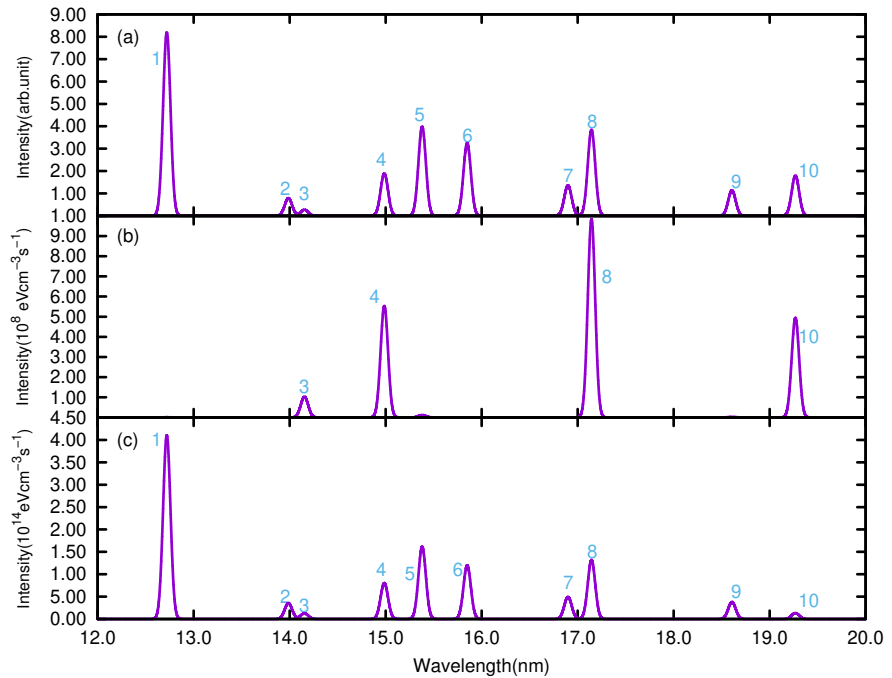


Fig. 1. The synthetic spectrum of W^{54+} ion in wavelength 12-20 nm. (a). Convoluting the transition rate with the Gaussian profile; (b). The spectrum for the EBIT case with the electron density $n_e = 10^{10} \text{ cm}^{-3}$ and the electron beam energy $E_e = 6000 \text{ eV}$; (c). The spectrum for the plasma with the electron density $n_e = 10^{16} \text{ cm}^{-3}$ and temperature $T_e = 6000 \text{ eV}$.

imental values and the synthetic spectrum provides a reasonable explanation for the EBIT experimental observation by the detailed analyse of the population mechanism. Finally, a new M1 transition with wavelength 14.154 nm were predicted that might be observed in the future EBIT experiment.

Acknowledgment

This work was supported by National Key Research and Development Program of China, Grant No:2017YFA0402300, National Nature Science Foundation of China, Grant No: 11264035, Specialized Research Fund for the Doctoral Program of Higher Education (SRFDP), Grant No: 20126203120004, International Scientific and Technological Cooperative Project of Gansu Province of China (Grant No. 1104WCGA186), JSPS-NRF-NSFC A3 Foresight Program in the field of Plasma Physics (NSFC: No. 11261140328, NRF: 2012K2A2A6000443).

References

References

- [1] G. Matthews, P. Coad, H. Greuner, M. Hill, T. Hirai, J. Likonen, H. Maier, M. Mayer, R. Neu, V. Philipps, R. Pitts, V. Riccardo, Development of divertor tungsten coatings for the JET ITER-like wall, *J. Nucl. Mater.* 390-391 (2009) 934-937. [doi:10.1016/j.jnucmat.2009.01.239](https://doi.org/10.1016/j.jnucmat.2009.01.239).
- [2] R. Neu, R. Dux, A. Kallenbach, T. Pütterich, M. Balden, J. Fuchs, A. Herrmann, C. Maggi, M. O'Mullane, R. Pugno, I. Radivojevic, V. Rohde, A. Sips, W. Sutrop, A. Whiteford, the ASDEX Upgrade team, Tungsten: an option for divertor and main chamber plasma facing components in future fusion devices, *Nucl. Fusion* 45 (2005) 209. [doi:10.1088/0029-5515/45/3/007](https://doi.org/10.1088/0029-5515/45/3/007).
- [3] R. Radtke, C. Biedermann, J. L. Schwob, P. Mandelbaum, R. Doron, Line and band emission from tungsten ions with charge 21+ to 45+ in the 45 – 70 Å range, *Phys. Rev. A* 64 (2001) 012720. [doi:10.1103/PhysRevA.64.012720](https://doi.org/10.1103/PhysRevA.64.012720).
- [4] C. H. Skinner, Atomic physics in the quest for fusion energy and ITER, *Phys. Scr. T134* (2009) 014022. [doi:10.1088/0031-8949/2009/T134/014022](https://doi.org/10.1088/0031-8949/2009/T134/014022).

[5] M. B. Chowdhuri, S. Morita, M. Goto, H. Nishimura, K. Nagai, S. Fujioka, Line analysis of EUV spectra from molybdenum and tungsten injected with impurity pellets in LHD, *Plasma Fusion Res.* 2 (2007) S1060–S1060. [doi:10.1585/pfr.2.S1060](https://doi.org/10.1585/pfr.2.S1060).

[6] X. Ding, I. Murakami, D. Kato, H. A. Sakaue, F. Koike, C. Dong, Collisional-radiative modeling of W^{27+} , *Plasma Fusion Res.* 7 (2012) 2403128–2403128. [doi:10.1585/pfr.7.2403128](https://doi.org/10.1585/pfr.7.2403128).

[7] A. Kramida, Recent progress in spectroscopy of tungsten, *Can. J. Phys.* 89 (2011) 551 – 570. [doi:10.1139/p11-045](https://doi.org/10.1139/p11-045).

[8] A. Kramida, T. Shirai, Energy levels and spectral lines of tungsten, W III through W LXXIV, *At. Data Nucl. Data Tables* 95 (2009) 305–474. [doi:10.1016/j.adt.2008.12.002](https://doi.org/10.1016/j.adt.2008.12.002).

[9] A. E. Kramida, J. Reader, Ionization energies of tungsten ions: W^{2+} through W^{71+} , *At. Data Nucl. Data Tables* 92 (2006) 457–479. [doi:10.1016/j.adt.2006.03.002](https://doi.org/10.1016/j.adt.2006.03.002).

[10] C. S. Harte, C. Suzuki, T. Kato, H. A. Sakaue, D. Kato, K. Sato, N. Tamura, S. Sudo, R. D’Arcy, E. Sokell, J. White, G. O’Sullivan, Tungsten spectra recorded at the lhd and comparison with calculations, *J. Phys. B: At., Mol. Opt. Phys.* 43 (2010) 205004. [doi:10.1088/0953-4075/43/i=20/a=205004](https://doi.org/10.1088/0953-4075/43/i=20/a=205004).

[11] J. Yanagibayashi, T. Nakano, A. Iwamae, H. Kubo, M. Hasuo, K. Itami, Highly charged tungsten spectra observed from JT-60U plasmas at $T_e \approx 8$ and 14 keV, *Journal of Physics B: Atomic, Molecular and Optical Physics* 43 (2010) 144013. [doi:10.1088/0953-4075/43/i=14/a=144013](https://doi.org/10.1088/0953-4075/43/i=14/a=144013).

[12] Z. Fei, W. Li, J. Grumer, Z. Shi, R. Zhao, T. Brage, S. Huldt, K. Yao, R. Hutton, Y. Zou, Forbidden-line spectroscopy of the ground-state configuration of Cd-like W, *Phys. Rev. A* 90 (2014) 052517. [doi:10.1103/PhysRevA.90.052517](https://doi.org/10.1103/PhysRevA.90.052517).

[13] I. Murakami, H. Sakaue, C. Suzuki, D. Kato, M. Goto, N. Tamura, S. Sudo, S. Morita, Development of quantitative atomic modeling for tungsten transport study using LHD plasma with tungsten pellet injection, *Nuclear Fusion* 55 (9) (2015) 093016. [doi:10.1088/0029-5515/55/9/093016](https://doi.org/10.1088/0029-5515/55/9/093016).

[14] Y. Ralchenko, I. N. Draganić, D. Osin, J. D. Gillaspy, J. Reader, Spectroscopy of diagnostically important magnetic-dipole lines in highly charged $3d^n$ ions of tungsten, *Phys. Rev. A* 83 (2011) 032517. [doi:10.1103/PhysRevA.83.032517](https://doi.org/10.1103/PhysRevA.83.032517).

[15] Y. Ralchenko, I. N. Draganic, J. N. Tan, J. D. Gillaspy, J. M. Pomeroy, J. Reader, U. Feldman, G. E. Holland, EUV spectra of highly-charged ions W^{54+} - W^{63+} relevant to ITER diagnostics, *J Phys B: At., Mol Opt Phys* 41 (2008) 021003. [doi:10.1088/0953-4075/41/2/021003](https://doi.org/10.1088/0953-4075/41/2/021003).

[16] X. Ding, S. Rui, K. Fumihiro, D. Kato, I. Murakami, H. A. Sakaue, C. Dong, Correlation, Breit and Quantum Electrodynamics effects on energy level and transition properties of W^{54+} ion, *Eur. Phys. J. D* 71 (2017) 73. [doi:10.1140/epjd/e2017-70829-y](https://doi.org/10.1140/epjd/e2017-70829-y).

[17] X. Ding, S. Rui, K. Fumihiro, I. Murakami, D. Kato, H. A. Sakaue, N. Nakamura, C. Dong, Energy levels, lifetimes and radiative data of W LV, *At. Data Nucl. Data Tables* 119 (2018) 354–425. [doi:10.1016/j.adt.2017.02.002](https://doi.org/10.1016/j.adt.2017.02.002).

[18] X. Ding, S. Rui, J. Liu, K. Fumihiro, I. Murakami, D. Kato, H. A. Sakaue, N. Nakamura, C. Dong, E1, M1, E2 transition energies and probabilities of W^{54+} ions, *J. Phys. B: At., Mol. Opt. Phys.* 50 (2017) 045004. [doi:10.1088/1361-6455/aa53ec](https://doi.org/10.1088/1361-6455/aa53ec).

[19] U. I. Safranova, A. S. Safranova, Wavelengths and transition rates for $nl-n'l'$ transitions in Be-, B-, Mg-, Al-, Ca-, Zn-, Ag- and Yb-like tungsten ions, *J. Phys. B: At., Mol. Opt. Phys.* 43 (2010) 074026. [doi:10.1088/0953-4075/43/7/074026](https://doi.org/10.1088/0953-4075/43/7/074026).

[20] P. Quinet, Dirac-Fock calculations of forbidden transitions within the $3p^k$ and $3d^k$ ground configurations of highly charged tungsten ions (W^{47+} - W^{61+}), *J. Phys. B: At., Mol. Opt. Phys.* 44 (2011) 195007. [doi:10.1088/0953-4075/44/19/195007](https://doi.org/10.1088/0953-4075/44/19/195007).

[21] X. L. Guo, M. Huang, J. Yan, S. Li, R. Si, C. Y. Li, C. Y. Chen, Y. S. Wang, Y. M. Zou, Relativistic many-body calculations on wavelengths and transition probabilities for forbidden transitions within the ground configurations in Co- through K-like ions of hafnium, tantalum, tungsten and gold, *J. Phys. B: At., Mol. Opt. Phys.* 48 (2015) 144020. [doi:10.1088/0953-4075/48/i=14/a=144020](https://doi.org/10.1088/0953-4075/48/i=14/a=144020).

[22] X. Ding, J. Liu, F. Koike, I. Murakami, D. Kato, H. A. Sakaue, N. Nakamura, C. Dong, Collisional-radiative model for the visible spectrum of W^{26+} ions, *Phys. Lett. A* 380 (2016) 874–877. [doi:10.1016/j.physleta.2015.12.034](https://doi.org/10.1016/j.physleta.2015.12.034).

[23] X. Ding, J. Yang, F. Koike, I. Murakami, D. Kato, H. A. Sakaue, N. Nakamura, C. Dong, Theoretical investigation on the soft X-ray spectrum of the highly-charged W^{54+} ions, *Journal of Quantitative Spectroscopy and Radiative Transfer* 204 (2018) 7 – 11. [doi:https://doi.org/10.1016/j.jqsrt.2017.08.020](https://doi.org/10.1016/j.jqsrt.2017.08.020).

[24] M. F. Gu, The Flexible Atomic Code, *Can. J. Phys.* 730 (2008) 127–136. [doi:10.1139/P07-197](https://doi.org/10.1139/P07-197).